

A new mixture model for spatiotemporal exceedances with flexible tail dependence

Ryan Li¹, Emily C. Hector^{1,2}, Brian J. Reich¹, and Reetam Majumder³

¹North Carolina State University

²University of Michigan

³University of Arkansas

Abstract

We propose a new model and estimation framework for spatiotemporal streamflow exceedances above a threshold that flexibly captures asymptotic dependence and independence in the tail of the distribution. We model streamflow using a mixture of processes with spatial, temporal and spatiotemporal asymptotic dependence regimes. A censoring mechanism allows us to use only observations above a threshold to estimate marginal and joint probabilities of extreme events. As the likelihood is intractable, we use simulation-based inference powered by random forests to estimate model parameters from summary statistics of the data. Simulations and modeling of streamflow data from the U.S. Geological Survey illustrate the feasibility and practicality of our approach.

Keywords: Spatial extremes, Censoring, Random forest, Simulation-based inference, Streamflow

1 Introduction

Flooding from extreme streamflow (water flow through rivers and streams) contributes to the more than \$179 billion annual cost in the United States (Joint Economic Committee Democrats, 2025). Flooding from streamflow can be mitigated through civil engineering solutions at appropriate locations along rivers and streams. For this reason, accurately and precisely modeling extreme streamflow events at high temporal resolution, such as daily streamflow maxima, has the potential to substantially limit the economic and human impacts of flooding. Extreme

streamflow, however, is difficult to model because the mechanics of flooding are complex, and extreme events are by definition rare.

Spatial extreme value analysis is a useful tool for modeling extreme streamflow because it allows the borrowing of information across sites to improve the accuracy and efficiency of estimates, and can allow extrapolation to unobserved sites. Max stable processes (MSPs) are a limiting class of models for block maxima (maximum values evaluated over a period of time) (Smith, 1990; Tawn, 1990; Schlather, 2002; Kabluchko et al., 2009; Wadsworth and Tawn, 2012; Reich and Shaby, 2012), making them a natural model for extreme streamflow measured at n locations. MSPs are typically used to model block maxima of spatio-temporal processes (e.g. annual maximum streamflow) across several time points (e.g. years) that are treated as independent replicates. This assumption of independence is violated at higher temporal resolutions, such as daily streamflow maxima, where a single flood event can be observed over multiple days. Further, a well-known characteristic of MSPs are their *asymptotic dependence* (Huser et al., 2025), wherein the conditional probability of observing an extreme event given another extreme event is strictly greater than zero or, mathematically, $\chi = \lim_{y \rightarrow \infty} P(Y_2 > y | Y_1 > y) > 0$. In practice, many environmental processes show decreasing spatial dependence in the tail of the distribution as events become more extreme. Interestingly, this does not guarantee asymptotic independence. Selecting a model with an incorrect tail dependence structure will result in poor extrapolation into the joint upper tails (Ledford and Tawn, 1996; Davison et al., 2013).

Models that can capture both asymptotic dependence *and* asymptotic independence are appealing alternatives to the restrictive tail dependence structure of the MSP. Examples include the max-mixture model of Wadsworth and Tawn (2012) and the copula-based mixture models in, e.g., Huser and Wadsworth (2019) and Majumder et al. (2024). These papers specify a copula for the dependence structure separately from the marginal models. Wadsworth and Tawn (2012) specify the copula as the maximum of two marginally Fréchet random variables, one with asymptotic dependence and one with asymptotic independence, while Huser and Wadsworth (2019) and Majumder et al. (2024) model the copula as a linear combination of an asymptotically dependent and an asymptotically independent process, to allow for flexible extremal dependence between two spatial locations. All three methods assume temporal independence, which makes them unsuitable for analyzing data observed at high temporal resolutions.

Recent work in this area aims to extend spatial extremes analysis to include temporal dependence. For example, Bortot and Gaetan (2024) extend the model in Huser and Wadsworth

(2019) to incorporate temporal dependence by modeling observations at each site over time with an autoregressive Gaussian time series; however, their model is limited to temporal asymptotic independence. Dell’Oro and Gaetan (2025) extend the Huser and Wadsworth (2019) model by allowing the mixture components to vary between temporal asymptotic dependence and independence, which allows for flexibility in temporal asymptotic properties for the model. This approach, however, requires an additional step to select the appropriate asymptotic dependence structures of the mixture components rather than letting the structure be chosen by the data. Maume-Deschamps et al. (2024) propose a max-mixture model with temporally varying mixture proportions which allows the model to vary between spatial asymptotic dependence and independence over time, but it cannot model temporal asymptotic dependence.

Exact inference for spatial extremes models in general and MSPs in particular pose significant computational challenges. Evaluating the density associated with a censored MSP is computationally intractable when n is even moderately large (Schlather, 2002; Wadsworth and Tawn, 2012; Wadsworth, 2015). For general MSPs, Castruccio et al. (2016) found full inference limited to $n = 13$ locations, while Huser et al. (2019) proposed an expectation-maximization algorithm for an MSP at $n = 20$ locations, with a computation time of 19.8 hours. Furthermore, exact inference is impossible for several variants of the scale-mixture model of Huser and Wadsworth (2019); this includes the models of Majumder et al. (2024) and Dell’Oro and Gaetan (2025) which are closely related to this work. There are two common approaches to address the intractability of spatial extremes models. The first involves the use of a composite likelihood approximations (Padoan et al., 2010; Huser et al., 2022). Composite likelihood suffers from statistical inefficiency for large n (Huser et al., 2016), finite-sample bias when using all pairs of observations (Sang and Genton, 2014; Wadsworth, 2015; Castruccio et al., 2016), and computational challenges posed by computing likelihoods at all $O(n^2)$ pairs. Simulation-based inference (SBI) has emerged as a popular alternative. SBI leverages the fact that while spatial extremes likelihoods might be challenging to evaluate, simulation from these processes is relatively straightforward. Broadly speaking, SBI can be categorized into methods to learn the likelihood (e.g., Majumder et al., 2024; Majumder and Reich, 2023; Walchessen et al., 2024), and methods to learn the posterior of parameters (e.g., Gerber and Nychka, 2021; Banesh et al., 2021; Sainsbury-Dale et al., 2024); we refer readers to Zammit-Mangion et al. (2025) for a recent review. For parameter estimation in particular, SBI proceeds by first generating a dense surface of plausible parameter values, and then generating data from the process for each set of parameter values. A predictive model (usually a deep learning model) is then trained to learn a

mapping from a set of carefully chosen summary statistics of the dataset to the parameters. This functions as a surrogate estimator that, when supplied with a dataset, can output the parameter values that the dataset is generated from. In spatial statistics, the approach was originally used to learn the parameters of the covariance matrix of a Gaussian process (Gerber and Nychka, 2021; Banesh et al., 2021); it has since been used for parameter estimation in a wide range of models of spatial extremes (Lenzi et al., 2023; Sainsbury-Dale et al., 2024; Richards et al., 2024; Hector and Lenzi, 2024; Dell’Oro and Gaetan, 2025; Sainsbury-Dale et al., 2025).

Our modeling framework has a product-sum correlation structure similar to the one outlined in De Cesare et al. (2001), which is a class of stationary spatio-temporal covariance functions used in the context of Gaussian models that are expressed as a weighted sum of spatial, temporal, and a product of spatial and temporal covariance functions. Gaussian models are not suitable for analysis of extreme data, as they are asymptotically independent and may not capture extremal dependence of observations. This structure is useful, however, due to its flexibility and guaranteed strict positive-definiteness (De Iaco et al., 2011). It has been used in analysis of stream network data (Bachrudin et al., 2023) which makes it a natural approach to expand on for this application.

Our contributions: We propose a new model and inferential framework that incorporates the flexibility of models proposed in Huser and Wadsworth (2019) and Majumder et al. (2024) with respect to extremal dependence, but that also incorporates a flexible model for temporal dependence. Relative to the two aforementioned works, our key idea is to introduce additional mixture components to the model that each represent asymptotic dependence or independence across space and/or time. Our model can therefore flexibly capture any of the four asymptotic (in)dependence regimes (space/time and independent/dependent), thereby improving prediction of daily streamflow maxima at unobserved sites and time points. Put into practice, our approach can improve the forecasting of extreme streamflow events at unobserved sites and present targeted locations and times for developing engineering solutions to prevent flood damage.

We use a peaks-over-threshold model for the marginal distribution of the data. This bears some resemblance to the approaches in Reich et al. (2013); Huser and Davison (2014); Hector and Reich (2024), where MSPs are used to model peaks over a threshold using a censored likelihood. Censoring observations below a threshold prevents non-extreme values from biasing our estimated model for the extremes. A major drawback of using more data and our more complex model is computational tractability. To overcome this computational difficulty, we use random forests (Breiman, 2001) trained on summary statistics of our data to estimate parameters

of our model. Notably, we use empirical χ_u values for pairs of observations as our predictors. Our use of random forests is a departure from the norm for SBI which has largely employed deep learning up until now. Deep learning is the popular choice due to its universality, but random forests are computationally cheaper and have fewer tuning parameters, making them preferable if there is minimal loss of accuracy and precision.

The remainder of the paper is organized as follows. Section 2 provides background on MSPs and tail dependence measures, and summarizes the mixture models of Huser and Wadsworth (2019) and Majumder et al. (2024). Section 3 describes our spatio-temporal model. Section 4 describes our proposed inferential framework for simulation based inference using random forests. Section 5 investigates model performance in terms of goodness-of-fit and inference through a simulation study. Section 6 analyzes daily streamflow maxima from U.S. Geological Survey (USGS) Hydro-Climatic Data Network (HCDN) stations to identify trends in extreme streamflow over the past 60 years using the proposed methods. Additional theoretical results are available in the Appendix. Data and code for the paper can be found at <https://github.com/rli2000/SpatialExtremeMixture>.

2 Background

2.1 χ -coefficient

Spatial and temporal dependence is often measured by the χ coefficient Coles (2001). Let $Y(s, t)$ denote a random process Y observed at spatial locations s and time points t . If we denote $q(\tau; s, t)$ as the τ quantile of $Y(s, t)$, then the χ coefficient between $Y(s, t)$ and $Y(s', t')$ is

$$\chi_\tau(s, t, s', t') = \text{Prob}[Y(s, t) > q(\tau; s, t) | Y(s', t') > q(\tau; s', t')], \quad (1)$$

$$\chi(s, t, s', t') = \lim_{\tau \rightarrow 1} \chi_\tau(s, t, s', t'). \quad (2)$$

For an isotropic process, we can write $\chi(h_S, h_T)$ for $h_S = ||s - s'||$ and $h_T = ||t - t'||$. The isotropic process Y is asymptotically dependent in space if $\chi(h_S, 0) > 0$; asymptotically dependent in time if $\chi(0, h_T) > 0$ for all s ; and asymptotically dependent in space and time if $\chi(h_S, h_T) > 0$ for all h_S and h_T .

2.2 Max-stable and inverted max-stable process

A stochastic process $\{Y_t, t \in T\}$, where T is an index set, is a max-stable process if, for some constants $A_{Nt} > 0, B_{Nt} : (N \geq 1, t \in T)$, and $Y_t^{(n)} : n = 1, \dots, N$ independent, identically distributed copies of Y_t , such that $Y_t^* = \{\max_{1 \leq n \leq N} Y_t^{(n)} - B_{nt}\}/A_{nt}$, then $\{Y_t^* : t \in T\} \stackrel{d}{=} \{Y_t, t \in T\}$ (Smith, 1990). This definition requires the marginal distribution of max-stable processes to be a generalized extreme value distribution. Max-stable processes are the infinite-dimensional generalization of multivariate extreme value theory (Smith, 1990), so they are a natural model for spatial extremes, which are infinite-dimensional extreme values.

A finite parametrization for the general max-stable process does not exist, so models are derived from a spectral representation (De Haan, 1984). Brown-Resnick processes are one such parametrized subclass of max-stable processes. A Brown-Resnick process can be defined as $Z(s) = \sup_{i \in \mathbb{N}} W_i(s)/T_i$, where $T_1 < T_2 < \dots$ are points of a Poisson process with rate 1, and $W_i(s)$ are copies of a random process $W(s) = \exp\{\epsilon(s) - \gamma(s)\}$, where $\epsilon(s)$ is a Gaussian process with semivariogram $\gamma(s)$ and $\epsilon(0) = 0$ almost surely (Brown and Resnick, 1977; Huser and Davison, 2013). The multivariate CDF for sites $s \in D$ is $P\{Z(s) < z(s), s \in D\} = \exp[-V_D\{z(s)\}]$, where $V_D\{z(s)\} = E\{\sup_{s \in D} W(s)/z(s)\}$, has explicit formula for $|D| \in \{1, 2\}$. This likelihood becomes computationally intractable for more than a few sites, requiring approximations such as composite likelihood or Vecchia approximation (Huser and Davison, 2013; Huser et al., 2022). Other families of max-stable models include the Schlather model (Schlather, 2002), and the extremal-t model (Brown and Resnick, 1977). Finally, if $Z(s)$ is a max-stable process with marginal CDF $G_s(x)$, then $W(s) = 1/G_s\{Z(s)\}$ has an inverted max-stable copula with Pareto margins (Wadsworth and Tawn, 2012; Ledford and Tawn, 1996). This process has positive association between pairs of observations, but asymptotic dependence.

2.3 Regression Trees and Random Forests

Regression trees are a machine learning tool that sequentially splits the training data into groups in a binary tree structure (Breiman et al., 2017). At each step, the training data is split to minimize $\sum_t \sum_{y_n \in t} \{y_n - \bar{y}(t)\}^2$, the sum of squared deviations across the two new groups. This process is repeated until the size of the resulting groups reaches a predefined lower bound, and then a pruning procedure is implemented to reduce the complexity of the tree. To predict the response value of a new observation, the leaf node corresponding to the new observation's predictor values is found, and the average response of training data in that node is taken as the prediction.

A random forest is an ensemble predictor consisting of k regression trees, $\{h(x, \Theta_i) : i = 1, \dots, k\}$, where $\{\Theta_i\}$ are independent, identically distributed random vectors, that averages the k predictions from the trees (Breiman, 2001). Each tree is grown from a subset of the response vector, Θ_i that is sampled from Y with replacement. This approach is popular for high-dimensional regression due to its power and interpretability (Meinshausen, 2006).

The tuning parameters for random forests are the number of trees k , and the length of the random vectors Θ_i , as well as the tuning parameters for the individual random tree predictors, the minimum group size.

3 Spatiotemporal mixture model

3.1 Tail model

We propose a model that extends the spatial mixture model in Huser and Wadsworth (2019) and Majumder et al. (2024) to the spatiotemporal setting to allow for asymptotic dependence or independence in space and/or time depending on model parameters. Let $i \in \{1, \dots, n\}$ index independent replicates (e.g., years), $t \in \mathcal{T}$ index correlated time points (e.g., days within year), and $s \in \mathcal{S} \subseteq \mathcal{R}^2$ denote the spatial location. The observations $Y_i(s, t)$ for $i \in \{1, \dots, n\}$, $t = \{1, \dots, T\}$, $s \in \{s_1, \dots, s_m\}$, are instances of the random process $Y(s, t)$ at time t and location s , whose joint distribution we describe below. We denote the marginal distribution of $Y(s, t)$ by $F(y; s, t)$. In our analysis of the streamflow data in Section 6, we assume that the upper tail of $F(\cdot; s, t)$ can be approximated by a generalized Pareto distribution (GPD) with parameters that vary across space and time; censoring is discussed in Section 4.

To model spatiotemporal dependence, we define a latent process $X(s, t)$ that is a transformation of the response, $Y(s, t) = G\{X(s, t); s, t\}$, where the transformation function $G(\cdot; s, t)$ is defined below. Note that since X and Y are one-to-one, they share asymptotic dependence properties as measured by $\chi(h_S, h_T)$. We model the latent process as a convex combination of four processes,

$$X(s, t) = \lambda_1 R_{ST}(s, t) + \lambda_2 R_S(s, t) + \lambda_3 R_T(s, t) + \lambda_4 W(s, t), \quad (3)$$

where R_{ST} , R_S , R_T and W each marginally follow standard exponential distributions and the mixture weights $\lambda = (\lambda_1, \dots, \lambda_4)$ satisfy $\lambda_k \geq 0$ and $\sum_{k=1}^4 \lambda_k = 1$. The four processes correspond to four distinct asymptotic regimes: R_{ST} is asymptotically dependent over space and time, R_S is asymptotically dependent over space but not time, R_T is asymptotically independent over

time but not space and W is asymptotically independent over space and time.

Specifically, R_{ST} , R_S and R_T are taken as max-stable processes and W is an inverted max-stable process, all marginally transformed to have standard exponential distributions. The spatiotemporal process R_{ST} is a Brown-Resnick process (Brown and Resnick, 1977; Kabluchko et al., 2009) with spatiotemporal correlation function

$$\exp\{-(h_S/\rho_S)^\alpha - (h_T/\rho_T)^\alpha\},$$

where h_S is the distance between two locations and h_T is the distance between two time points. The spatial Brown-Resnick process R_S has spatial variogram $(h_S/\rho_S)^\alpha$ and is completely independent over time. Similarly, the temporal Brown-Resnick process R_T has temporal variogram $(h_T/\rho_T)^\alpha$ and is independent over space. Finally, W is an inverted Brown-Resnick process (Wadsworth and Tawn, 2012) with spatial variogram $(h_S/\rho_S)^\alpha + (h_T/\rho_T)^\alpha$, which is asymptotically independent over space and time.

The marginal distribution of $X(s, t)$ for all s and t is the hypoexponential distribution with parameters $(\lambda_1, \lambda_2, \lambda_3, \lambda_4)$ and cumulative distribution function

$$H_\lambda(x) = 1 - \left(\prod_{k=1}^4 \lambda_k^{-1} \right) \sum_{j=1}^4 \left[\left\{ -\lambda_j^{-1} \prod_{k \neq j} (\lambda_k^{-1} - \lambda_j^{-1}) \right\}^{-1} e^{-x/\lambda_j} \right], \quad (4)$$

for distinct $\lambda_1, \dots, \lambda_4$. We therefore use $G(x; s, t) = F^{-1}\{H_\lambda(x); s, t\}$ to relate the latent process $X(s, t)$ to the response $Y(s, t) = G\{X(s, t); s, t\}$. By construction, the process $Y(s, t)$ has marginal distribution function $F(\cdot; s, t)$ and inherits the spatiotemporal dependence properties of $X(s, t)$.

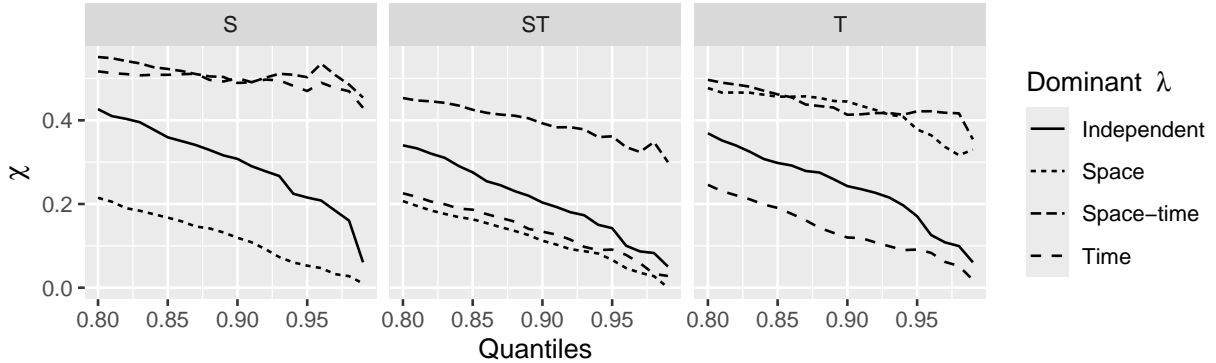
To simplify the model, we assume the spatial and temporal range parameters ρ_S and ρ_T are constant across all four mixture components, and the smoothness parameter is fixed at $\alpha = 1$. Since the interpretation of ρ_S is the same across all four mixture components, we can treat it as the overall spatial range for the process $X(s, t)$, and likewise for ρ_T . This gives spatial dependence parameters $\theta = (\lambda_1, \lambda_2, \lambda_3, \lambda_4, \rho_S, \rho_T)$. Using this model, we can capture any combination of spatial and temporal asymptotic dependence regimes by varying θ , as shown in Section 3.2.

3.2 Asymptotic tail dependence

We study the asymptotic dependence structure of a simplified version of the process in equation (3) given by

$$X(s, t) = \lambda_1 R_1 + \lambda_2 R_2(t) + \lambda_3 R_3(s) + \lambda_4 R_4(s, t), \quad (5)$$

Figure 1: Empirical χ plots for four λ settings for $X(s, t), X(s', t)$ (left), $X(s, t), X(s', t')$ (middle) and $X(s, t), X(s, t')$ (right).



where R_1 , $R_2(t)$, $R_3(s)$ and $R_4(s, t)$ all follow mutually independent standard exponential distributions. This simplifies derivations but maintains the key dependence properties of each component; for example, $R_2(t)$ is constant in s and thus dependent across space but not time. We further assume that the $\lambda_1, \dots, \lambda_4$ are distinct and denote $j = \arg \max_k \lambda_k$ as the dominant term. The following Theorem 1 shows that the simplified model of (5) is sufficiently flexible to account for (a) spatial, (b) temporal and (c) spatiotemporal dependence, and that inference on the dominant term j provides a way to distinguish between these modes of dependence.

Theorem 1 *Under the model in (5):*

- (a) $X(s, t)$ and $X(s', t)$ are asymptotically dependent if and only if $j \in \{1, 2\}$,
- (b) $X(s, t)$ and $X(s, t')$ are asymptotically dependent if and only if $j \in \{1, 3\}$,
- (c) $X(s, t)$ and $X(s', t')$ are asymptotically dependent if and only if $j = 1$.

A proof is provided in Appendix A.

While the derivations for the full model in (3) are cumbersome, we explore results analogous to Theorem 1 for the full model graphically in Figure 1. We generate 10,000 draws from the mixture model with parameters $\rho_S = \rho_T = 0.2$ at four spatio-temporal locations: $(0, 0, 0)$, $(0.8, 0, 0)$, $(0, 0, 0.4)$, $(0.8, 0, 0.4)$. Each model has dominant $\lambda_j = 0.4$, and remaining terms $\lambda_k \approx 0.2$, with minor perturbations to maintain distinct values. The empirical results support the conclusion of the theorem for the model in (3); for two spatial sites, $\chi_u \rightarrow 0$ when $j \in \{3, 4\}$ and otherwise χ_u approaches a larger value, indicating likely asymptotic dependence. Similar results follow for two points separated in time, and separated in both space and time.

4 Parameter estimation

4.1 Marginal parameter estimates

We first transform the data to standard uniform margins before estimating the dependence parameters θ . We do this by modeling the marginal distribution of the data and performing a probability integral transformation. Since we are modeling with a points-above-threshold approach, we model the marginal distribution of our data with a Generalized Pareto distribution with threshold taken to be the q_0 marginal quantile for each spatial location. We use maximum likelihood estimation (MLE) to estimate marginal parameters, with one shared shape parameter and separate range parameters for each spatial location. The observations $Y_i(s, t)$ are then transformed to $U_i(s, t) \in [0, 1]$ using the fitted distribution function; observations below the threshold can be set to any value below the threshold because, as described below, they do not affect the estimation of θ .

4.2 Dependence parameter estimates

One challenge in using full likelihood inference to estimate our model is to evaluate the likelihood. Indeed, the max-stable processes in our mixture model have a computationally intractable full likelihood for more than a small number of observations. This computational problem is exacerbated by censoring of observations in our peaks over threshold analysis. As it is straightforward to simulate data from the model, we instead use SBI for parameter estimation.

First, we generate S draws from the prior distribution of the parameters. To work in an unbounded domain, we apply the following transformation: $\eta_1 = \log(\lambda_2/\lambda_1)$, $\eta_2 = \log(\lambda_3/\lambda_1)$, $\eta_3 = \log(\lambda_4/\lambda_1)$, $\eta_4 = \log \rho_S$ and $\eta_5 = \log \rho_T$. The prior distributions are $\eta_j \sim \text{Normal}(m_j, s_j^2)$, $j = 1, \dots, 5$. For each of the S parameter sets, we draw a dataset from the model using the same spatiotemporal locations and number of independent replicates as the dataset to be analyzed. The datasets are then reduced to summary statistics, Z , as described below. We then use the S samples to train a random forest model for each parameter, $\hat{\eta}_j = \hat{f}_j(Z)$, $j = 1, \dots, 5$. To estimate a parameter given a real dataset, we simply compute the summary statistics for the real dataset and pass them through the fitted model \hat{f}_j , $j = 1, \dots, 5$. For uncertainty quantification, we use non-parametric bootstrap (i.e., replications sampled with replacement) to derive both estimates of standard errors and parameter confidence intervals.

The summary statistics are derived from empirical versions of the χ coefficients in (1). We compute $\hat{\chi}_\tau(s, t, s', t')$ for thresholds $\tau \in \{q_1, \dots, q_m\}$ across all pairs of spatiotemporal

locations. Of course, the thresholds q_j should be at least as large as the marginal threshold, q_0 . Separately by τ , the empirical χ coefficients are binned over spatial and temporal distance. We bin observations by every 0.1 increment in spatial or temporal distance (with each spatiotemporal dimension scaled to $[0, 1]$), with five spatial bins and three temporal bins, and then smoothed using a 2D B-spline to reduce noise in the model inputs. In the simulation study of Section 5 we use $m = 2$, $q_1 = 0.5$ and $q_2 = 0.9$, but in practice this will require tuning. Additionally, we consider the statistic $\text{corr}\{U(s, t), U(s', t')|U(s, t) > q_0, U(s', t') > q_0\}$. Since we consider only values above 0.5 in the correlation calculation, we effectively censor the data at the 0.5 quantile level because data below the threshold will not affect our estimates. Given the summary statistics, the regression functions \hat{f}_j are fitted using the S parameters/summary statistic pairs using random forest with default settings in the `quantregForest` package (Meinshausen, 2006), separately across parameters η_1, \dots, η_5 .

Finally, we transform from η to θ using the inverse transformations: $\lambda_1 = 1/\{\sum_{i=0}^3 \exp(\eta_i)\}$, $\lambda_2 = \exp(\eta_1)/\{\sum_{i=0}^3 \exp(\eta_i)\}$, $\lambda_3 = \exp(\eta_2)/\{\sum_{i=0}^3 \exp(\eta_i)\}$, $\lambda_4 = \exp(\eta_3)/\{\sum_{i=0}^3 \exp(\eta_i)\}$, $\rho_S = \exp \eta_4$, and $\rho_T = \exp \eta_5$, where $\eta_0 = 0$. We apply this transformation to the estimates before computing bootstrap confidence intervals.

5 Simulation experiments

We investigate the properties of our model and estimation procedure through numerical experiments on simulated data. The spatio-temporal domain $\mathcal{T} \times \mathcal{S}$ is a three-dimensional unit cube and observations are sampled on a uniform grid of dimension $5 \times 5 \times 5$. That is, $t \in \{1, \dots, 5\}$ and $s \in \{(a, b)\}_{a,b=1}^5$ such that $T = 5, m = 25$. We construct four settings where λ_i is the dominant term for each $i \in \{1, 2, 3, 4\}$. In the setting where λ_i is dominant, $\lambda_i = 0.5, \lambda_j \in \{0.15, 0.17, 0.18\}$ for $j \neq i$; the remaining λ_j are assigned values based on index order. In all scenarios and settings, the spatial and temporal range values are $\rho_S = \rho_T = 0.4$, and the marginal shape and scale parameters are 0.2 and 1, respectively. The scale parameters are estimated individually for each of the 25 sites, but for brevity only σ_1 , the scale at location 1, is reported. For each setting, we run 100 simulations. In all scenarios, the number of independent replicates is $n = 100$. Parameter estimation is carried out using the random forest approach described in Section 4.

Table 1 shows that our model estimates the λ parameters very well. The bias is generally low and the coverage is near the nominal level and in these synthetic cases we are able to consistently identify the asymptotic regime. Additionally, the range parameters ρ_S and ρ_T are reasonably estimated in most cases, although bias and low coverage is observed when data are generated

with strong asymptotic dependence.

Parameter	True	Mean	Bias	RMSE	SE	Coverage
λ_1	0.500	0.467	0.091	0.008	0.085	0.84
λ_2	0.150	0.122	0.059	0.003	0.052	0.89
λ_3	0.170	0.178	0.045	0.002	0.045	1.00
λ_4	0.180	0.233	0.116	0.013	0.103	0.91
ρ_S	0.400	0.581	0.213	0.045	0.112	0.75
ρ_T	0.400	0.534	0.156	0.024	0.081	0.77
ξ	0.200	0.163	-0.036	0.172	0.119	
σ	1.000	1.125	0.125	0.101	0.095	

(a) Asymptotic spatiotemporal dependence with $\lambda_1 = 0.5$

Parameter	True	Mean	Bias	RMSE	SE	Coverage
λ_1	0.150	0.127	0.034	0.001	0.024	0.88
λ_2	0.500	0.446	0.074	0.005	0.051	0.97
λ_3	0.170	0.223	0.080	0.006	0.060	0.97
λ_4	0.180	0.204	0.083	0.007	0.080	0.94
ρ_S	0.400	0.419	0.049	0.002	0.046	0.98
ρ_T	0.400	0.250	0.163	0.027	0.064	0.34
ξ	0.200	0.190	-0.010	0.047	0.046	
σ	1.000	1.098	0.098	0.127	0.081	

(b) Asymptotic spatial dependence with $\lambda_2 = 0.5$

Parameter	True	Mean	Bias	RMSE	SE	Coverage
λ_1	0.150	0.118	0.038	0.001	0.021	0.85
λ_2	0.170	0.199	0.062	0.004	0.056	0.97
λ_3	0.500	0.510	0.041	0.002	0.040	0.98
λ_4	0.180	0.173	0.048	0.002	0.047	0.89
ρ_S	0.400	0.406	0.149	0.022	0.150	0.97
ρ_T	0.400	0.408	0.039	0.002	0.038	0.95
ξ	0.200	0.191	-0.009	0.032	0.031	
σ	1.000	1.063	0.063	0.088	0.061	

(c) Asymptotic temporal dependence with $\lambda_3 = 0.5$

Parameter	True	Mean	Bias	RMSE	SE	Coverage
λ_1	0.150	0.189	0.078	0.006	0.068	0.92
λ_2	0.170	0.149	0.044	0.002	0.039	0.93
λ_3	0.180	0.214	0.067	0.004	0.057	0.89
λ_4	0.500	0.448	0.131	0.017	0.120	0.90
ρ_S	0.400	0.452	0.119	0.014	0.107	0.97
ρ_T	0.400	0.414	0.068	0.005	0.066	0.94
ξ	0.200	0.187	-0.013	0.044	0.042	
σ	1.000	1.092	0.092	0.133	0.097	

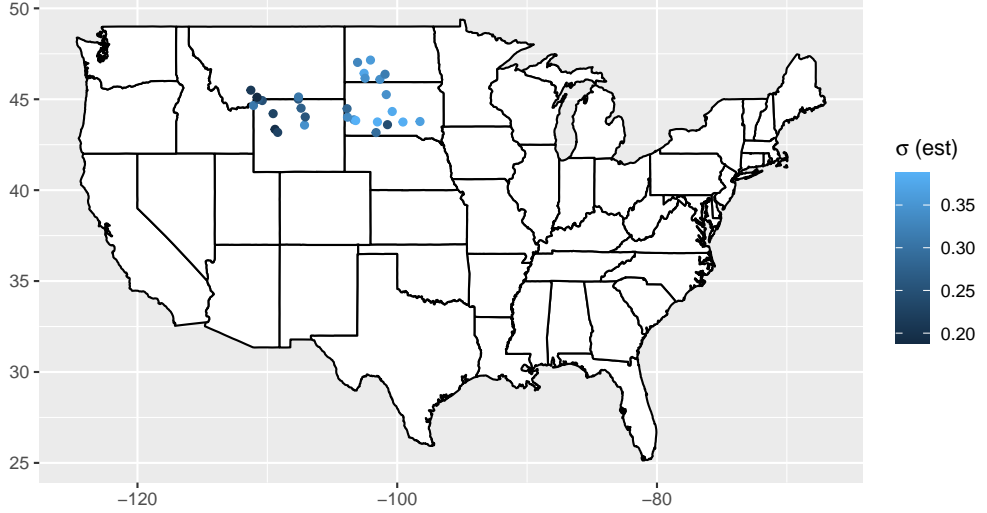
(d) Asymptotic independence with $\lambda_4 = 0.5$

Table 1: Parameter estimates when asymptotic dependence is (a) spatio-temporal, (b) spatial, (c) temporal and (d) independent. The parameters λ_j control the type of dependence; ρ_S and ρ_T are the spatial and temporal range parameters and ξ and σ are the marginal scale and shape parameters. “Coverage” refers to the empirical coverage of 95% bootstrap confidence intervals.

6 Analysis of extreme streamflow

We illustrate our method using daily streamflow data downloaded from the USGS Hydro-Climatic Data Network (HCDN; Lins, 2012). We focus on the $m = 30$ stations in the western/midwestern US; these are mapped in Figure 2 in USGS hydrologic unit codes region 10U and the $n = 60$ years from 1965 to 2024. The spatiotemporal coordinates are projected onto the unit cube. Because the vast majority of extreme values occur in the summer, we restrict our analysis to data from May to July. The data is downloaded using the `dataRetrieval` package

Figure 2: Scale parameter estimates across space



in **R** (De Cicco et al., 2022). The objectives of the analysis are to estimate the marginal return levels at each site and test for asymptotic spatial and temporal dependence.

We first transform the raw data by taking its square root, which reduces the extreme heavy-tailedness for numerical stability. We then harmonize the data across stations by defining the response for year $i \in \{1, \dots, n\}$ for the station at spatial location s and day of the year $t \in \{1, \dots, T\}$ as

$$Y_i(s, t) = \frac{Z_i(s, t) - q_{0.5}(s)}{q_{0.9}(s) - q_{0.1}(s)}, \quad (6)$$

where $Z_i(s, t)$ is the square root of the original measurement and $q_\tau(s)$ is the sample τ quantile of the observations at location s . We then assume the marginal distribution is

$$Y_i(s, t) | Y_i(s, t) > Q_\tau \sim \text{GPD}\{Q_\tau, \sigma_i(s), \xi(s)\}, \quad (7)$$

where the threshold Q_τ is the empirical τ quantile of the data pooled across time at each location and $\sigma_i(s), \xi(s)$ are location-specific maximum likelihood estimates for the GPD parameter. Estimation is carried out using the **eva** package (Bader and Yan, 2020) based on the entire data, ignoring spatial and temporal dependence. The QQ-plot in Figure 3 shows the GPD model fits the data well for $\tau = 0.8$, which we use for the remainder of the analysis.

The parameter estimates are reported in Table 2. Mixture parameter λ_4 was estimated as the largest, indicating that the data is asymptotically independent in both space and time. There is, however, significant weight in λ_1 , which indicates a component with asymptotic dependence in

Figure 3: QQ plot of marginal fits of streamflow data at thresholds $\tau = 0.5, 0.8, 0.9, 0.95$.

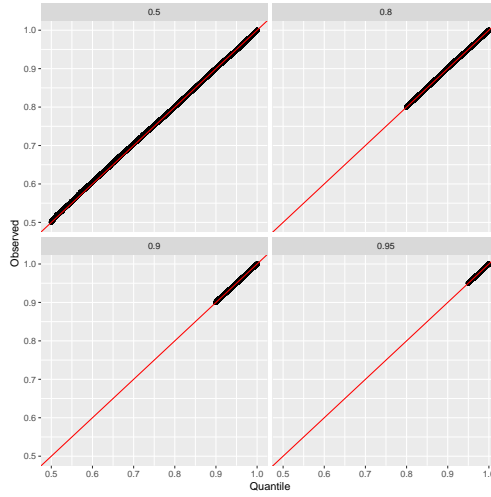
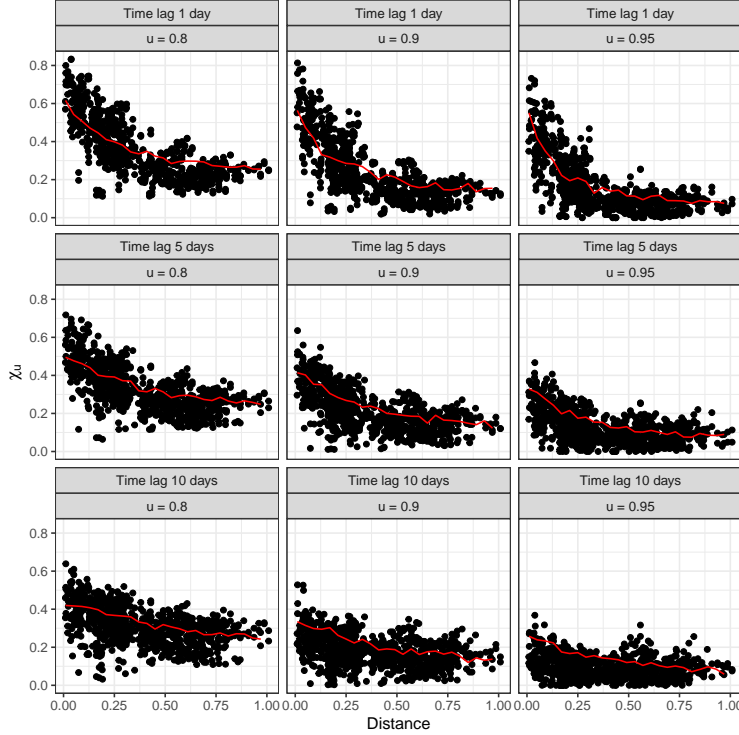


Table 2: Parameter Estimates and 95% Bootstrap CIs

Parameter	Estimate	95% CI
λ_1	0.134	(0.114, 0.174)
λ_2	0.063	(0.054, 0.139)
λ_3	0.268	(0.150, 0.302)
λ_4	0.534	(0.485, 0.625)
ρ_S	0.261	(0.214, 0.462)
ρ_T	0.244	(0.221, 0.341)

Figure 4: Empirical χ statistics for pairs of stations plotted against distance for different temporal lags (right) for each station. The red line indicates χ statistics for fitted model.



space-time. Over 1000 non-parametric bootstrap samples, all 1000 resulted in λ_4 being largest, indicating strong evidence that the data is asymptotically independent in space and time.

Figure 4 plots the empirical χ_u values against (normalized) distance in space, for $u = 0.8, 0.9, 0.95$ and time lags of 1, 5, and 10 days. The red line is a plot of approximate χ_u generated from our model at the fitted values. The modeled line matching the trend of the empirical χ_u from the data indicates that our model fit accurately reflects the pairwise asymptotic behavior of the real data across space-time. We can also see that $\chi_u \rightarrow 1 - u$ as distance increases, indicating our model captures independence as spatial distance increases.

The estimated ρ_S and ρ_T parameters are 0.261 and 0.244 respectively, indicating that spatial dependence is limited to about 1/4 of our spatial domain and that temporal dependence is limited to about 15 days. The diagnostic plots in Figure 4 show that the fitted spatiotemporal dependence functions matches the empirical χ coefficients and thus that the model fits the data well. From the scale parameters plotted in Figure 2, we see that, across the spatial domain of interest, streamflow is higher for sites in the eastern portion of our spatial domain.

7 Discussion

In this paper, we proposed a process mixture model for spatial extremes whose spatio-temporal dependence is characterized by a convex combination of four random variables of differing asymptotic dependence. This model extends Huser and Wadsworth (2019) and Majumder et al. (2024) to include temporal dependence. Marginal parameters are estimated using standard maximum likelihood estimation, and dependence parameters are estimated using random forest regression. We use this model to analyze daily streamflow data in the Western/Midwestern United States. We find that, over this domain, daily streamflow data is asymptotically independent over space and time.

Future work will focus on improving estimation of model parameters. Although our results demonstrate that random forest regression is sufficient for estimation, estimating all parameters simultaneously may improve efficiency of uncertainty quantification, either with approximate likelihood approaches or a neural network approach. Additionally, estimating marginal parameters and dependence parameters simultaneously may improve efficiency for estimating marginal parameters as well. This model cannot make predictions at unobserved sites, both in space and in time; for applications like extreme streamflow, it may be useful to investigate whether it is possible to adapt this model to allow for prediction, so forecasts can be made to inform flood response policy. Finally, we hope to expand on the theoretical properties of the model. Although this paper derives χ for the model for different values of λ in complete dependence and independence cases, it does not cover the general case where R and W are spatio-temporal processes.

Acknowledgements

This work was supported by National Science Foundation grants DMS2152887 and CBET2151651. The authors also thank Dr. Sankar Arumugam of North Carolina State University for providing and describing the streamflow data.

References

Bachrudin, A., Ruchjana, B. N., Abdullah, A. S., and Budiarto, R. (2023). Spatio-temporal model of a product–sum simulation on stream network based on hydrologic distance. *Water*, 15(11):2039.

Bader, B. and Yan, J. (2020). *EVA: Extreme Value Analysis with Goodness-of-Fit Testing*. R package version 0.2.6.

Banesh, D., Panda, N., Biswas, A., Roekel, L. V., Oyen, D., Urban, N., Grosskopf, M., Wolfe, J., and Lawrence, E. (2021). Fast gaussian process estimation for large-scale in situ inference using convolutional neural networks. In *2021 IEEE International Conference on Big Data (Big Data)*, pages 3731–3739.

Bortot, P. and Gaetan, C. (2024). A model for space-time threshold exceedances with an application to extreme rainfall. *Statistical Modelling*, 24(2):169–193.

Breiman, L. (2001). Random forests. *Machine Learning*, 45(1):5–32.

Breiman, L., Friedman, J. H., Olshen, R. A., and Stone, C. J. (2017). *Classification And Regression Trees*. Routledge, UK.

Brown, B. M. and Resnick, S. I. (1977). Extreme values of independent stochastic processes. *Journal of Applied Probability*, 14(4):732–739.

Castruccio, S., Huser, R., and Genton, M. G. (2016). High-order composite likelihood inference for max-stable distributions and processes. *Journal of Computational and Graphical Statistics*, 25(4):1212–1229.

Coles, S. (2001). *An Introduction to Statistical Modeling of Extreme Values*. Springer, London.

Davison, A. C., Huser, R., and Thibaud, E. (2013). Geostatistics of dependent and asymptotically independent extremes. *Mathematical Geosciences*, 45:511–529.

De Cesare, L., Myers, D., and Posa, D. (2001). Estimating and modeling space–time correlation structures. *Statistics & Probability Letters*, 51(1):9–14.

De Cicco, L. A., Lorenz, D., Hirsch, R. M., Watkins, W., and Johnson, M. (2022). *dataRetrieval: R packages for discovering and retrieving water data available from U.S. federal hydrologic web services*. Reston, VA.

De Haan, L. (1984). A spectral representation for max-stable processes. *The Annals of Probability*, pages 1194–1204.

De Iaco, S., Myers, D., and Posa, D. (2011). On strict positive definiteness of product and product–sum covariance models. *Journal of Statistical Planning and Inference*, 141(3):1132–1140.

Dell'Oro, L. and Gaetan, C. (2025). Flexible space–time models for extreme data. *Spatial Statistics*, 68:100916.

Gerber, F. and Nychka, D. (2021). Fast covariance parameter estimation of spatial gaussian process models using neural networks. *Stat*, 10(1):e382.

Hector, E. C. and Lenzi, A. (2024). When the whole is greater than the sum of its parts: Scaling black-box inference to large data settings through divide-and-conquer. *arXiv preprint arXiv:2412.20323*.

Hector, E. C. and Reich, B. J. (2024). Distributed inference for spatial extremes modeling in high dimensions. *Journal of the American Statistical Association*, 119(546):1297–1308.

Huser, R. and Davison, A. C. (2013). Composite likelihood estimation for the Brown–Resnick process. *Biometrika*, 100(2):511–518.

Huser, R. and Davison, A. C. (2014). Space–time modelling of extreme events. *Journal of the Royal Statistical Society, Series B*, 76(2):439–461.

Huser, R., Davison, A. C., and Genton, M. G. (2016). Likelihood estimators for multivariate extremes. *Extremes*, 19(1):79–103.

Huser, R., Dombry, C., Ribatet, M., and Genton, M. G. (2019). Full likelihood inference for max-stable data. *Stat*, 8(1):e218.

Huser, R., Opitz, T., and Wadsworth, J. L. (2025). Modeling of spatial extremes in environmental data science: time to move away from max-stable processes. *Environmental Data Science*, 4:e3.

Huser, R., Stein, M. L., and Zhong, P. (2022). Vecchia likelihood approximation for accurate and fast inference in intractable spatial extremes models. *arXiv preprint arXiv:2203.05626*.

Huser, R. and Wadsworth, J. L. (2019). Modeling spatial processes with unknown extremal dependence class. *Journal of the American Statistical Association*, 114(525):434–444.

Joint Economic Committee Democrats (2025). Flooding costs the U.S. between \$179.8 and \$496.0 billion each year. *Publications*, <https://www.jec.senate.gov/public/index.cfm/democrats/2024/6/flooding-costs-the-u-s-between-179-8-and-496-0-billion-each-year>. [Online; accessed 18 March 2025].

Kabluchko, Z., Schlather, M., and de Haan, L. (2009). Stationary max-stable fields associated to negative definite functions. *The Annals of Probability*, 37(5):2042 – 2065.

Ledford, A. W. and Tawn, J. A. (1996). Statistics for near independence in multivariate extreme values. *Biometrika*, 83(1):169–187.

Lenzi, A., Bessac, J., Rudi, J., and Stein, M. L. (2023). Neural networks for parameter estimation in intractable models. *Computational Statistics & Data Analysis*, 185:107762.

Lins, H. F. (2012). USGS Hydro-Climatic Data Network 2009 (HCDN-2009). *US Geological Survey Fact Sheet*, 3047(4).

Majumder, R. and Reich, B. J. (2023). A deep learning synthetic likelihood approximation of a non-stationary spatial model for extreme streamflow forecasting. *Spatial Statistics*, 55:100755.

Majumder, R., Reich, B. J., and Shaby, B. A. (2024). Modeling extremal streamflow using deep learning approximations and a flexible spatial process. *The Annals of Applied Statistics*, 18(2):1519–1542.

Maume-Deschamps, V., Ribereau, P., and Zeidan, M. (2024). A spatio-temporal model for temporal evolution of spatial extremal dependence. *Spatial Statistics*, 64:100860.

Meinshausen, N. (2006). Quantile regression forests. *J. Mach. Learn. Res.*, 7:983–999.

Padoan, S., Ribatet, M., and Sisson, S. (2010). Likelihood-based inference for max-stable processes. *Journal of the American Statistical Association*, 105(489):263–277.

Reich, B. J. and Shaby, B. A. (2012). A hierarchical max-stable spatial model for extreme precipitation. *The Annals of Applied Statistics*, 6(4):1430.

Reich, B. J., Shaby, B. A., and Cooley, D. (2013). A hierarchical model for serially-dependent extremes: a study of heat waves in the western US. *Journal of Agricultural, Biological and Environmental Statistics*, 19(1):119–135.

Richards, J., Sainsbury-Dale, M., Zammit-Mangion, A., and Huser, R. (2024). Neural Bayes estimators for censored inference with peaks-over-threshold models. *Journal of Machine Learning Research*, 25(390):1–49.

Sainsbury-Dale, M., Zammit-Mangion, A., and Huser, R. (2024). Likelihood-free parameter estimation with neural Bayes estimators. *The American Statistician*, 78(1):1–14.

Sainsbury-Dale, M., Zammit-Mangion, A., Richards, J., and Huser, R. (2025). Neural Bayes estimators for irregular spatial data using graph neural networks. *Journal of Computational and Graphical Statistics*, 34(3):1153–1168.

Sang, H. and Genton, M. G. (2014). Tapered composite likelihood for spatial max-stable models. *Spatial Statistics*, 8:86–103.

Schlather, M. (2002). Models for stationary max-stable random fields. *Extremes*, 5:33–44.

Smith, R. L. (1990). Max-stable processes and spatial extremes. *Unpublished manuscript*, 205:1–32.

Tawn, J. A. (1990). Modelling multivariate extreme value distributions. *Biometrika*, 77(2):245–253.

Wadsworth, J. L. (2015). On the occurrence times of componentwise maxima and bias in likelihood inference for multivariate max-stable distributions. *Biometrika*, 102(3):705–711.

Wadsworth, J. L. and Tawn, J. A. (2012). Dependence modelling for spatial extremes. *Biometrika*, pages 253–272.

Walchessen, J., Lenzi, A., and Kuusela, M. (2024). Neural likelihood surfaces for spatial processes with computationally intensive or intractable likelihoods. *Spatial Statistics*, 62:100848.

Zammit-Mangion, A., Sainsbury-Dale, M., and Huser, R. (2025). Neural methods for amortized inference. *Annual Review of Statistics and Its Application*, 12(Volume 12, 2025):311–335.

Appendix – Proof of Theorem 1

Let $X_1 = X(s_1, t_1), X_2 = X(s_2, t_2)$ be the value of the process at two spatio-temporal locations.

Consider the joint survival function of $X_1, X_2, P(X_1 > y, X_2 > y)$, in 3 cases.

Case 1: $s_1 \neq s_2, t_1 = t_2$

Let $t = t_1 = t_2$. We have $R_2(t_1) = R_2(t_2) = R_2$ so $X_1 = \lambda_1 R_1 + \lambda_2 R_2 + \lambda_3 R_3(s_1) + \lambda_4 W(s_1, t)$, $X_2 = \lambda_1 R_1 + \lambda_2 R_2 + \lambda_3 R_3(s_2) + \lambda_4 W(s_2, t)$.

Then, for $P(X_1 > y, X_2 > y)$, we have the following:

$$\begin{aligned}
P(X_1 > y, X_2 > y) &= P(\lambda_1 R_1 + \lambda_2 R_2 + \lambda_3 R_3(s_1) + \lambda_4 W(s_1, t) > y, \\
&\quad \lambda_1 R_1 + \lambda_2 R_2 + \lambda_3 R_3(s_2) + \lambda_4 W(s_2, t) > y) \\
&= E_{R_2}[E_{R_1}\{P(\lambda_3 R_3(s_1) + \lambda_4 W(s_1, t) > y - \lambda_1 r_1 - \lambda_2 r_2, \\
&\quad \lambda_3 R_3(s_2) + \lambda_4 W(s_2, t) > y - \lambda_1 r_1 - \lambda_2 r_2 | R_1 = r_1, R_2 = r_2)\}] \\
&= E_{R_2}[E_{R_1}\{P(\lambda_3 R_3(s_1) + \lambda_4 W(s_1, t) > y - \lambda_1 r_1 - \lambda_2 r_2 | R_1 = r_1, R_2 = r_2) \\
&\quad P(\lambda_3 R_3(s_2) + \lambda_4 W(s_2, t) > y - \lambda_1 r_1 - \lambda_2 r_2 | R_1 = r_1, R_2 = r_2)\}]
\end{aligned}$$

where we used the independence of $R_3(s_1), R_3(s_2), W(s_1, t)$, and $W(s_2, t)$ to get the last line.

Since $\lambda_3 R_3(s_1) + \lambda_4 W(s_1, t)$ follows a hypoexponential distribution with parameters λ_3, λ_4 , we know $P(\lambda_3 R_3(s_1) + \lambda_4 W(s_1, t) > x) = \frac{\lambda_3}{\lambda_3 - \lambda_4} \exp(-x/\lambda_3) - \frac{\lambda_4}{\lambda_3 - \lambda_4} \exp(-x/\lambda_4)$ if $x > 0$, and 1 otherwise. Thus, equation (1) simplifies to:

$$\begin{aligned}
P(X_1 > y, X_2 > y) &= E_{R_1}[E_{R_2}\{P(\lambda_3 R_3(s_1) + \lambda_4 W(s_1, t) > y - \lambda_1 r_1 - \lambda_2 r_2 | R_1 = r_1, R_2 = r_2) \\
&\quad \cdot P(\lambda_3 R_3(s_2) + \lambda_4 W(s_2, t) > y - \lambda_1 r_1 - \lambda_2 r_2 | R_1 = r_1, R_2 = r_2) I(\lambda_1 r_1 + \lambda_2 r_2 > y)\}] \\
&\quad + E_{R_1}[E_{R_2}\{P(\lambda_3 R_3(s_1) + \lambda_4 W(s_1, t) > y - \lambda_1 r_1 - \lambda_2 r_2 | R_1 = r_1, R_2 = r_2) \\
&\quad \cdot P(\lambda_3 R_3(s_2) + \lambda_4 W(s_2, t) > y - \lambda_1 r_1 - \lambda_2 r_2 | R_1 = r_1, R_2 = r_2) I(\lambda_1 r_1 + \lambda_2 r_2 \leq y)\}] \\
&= P(\lambda_1 R_1 + \lambda_2 R_2 > y) \\
&\quad + E_{R_1}[E_{R_2}\{P(\lambda_3 R_3(s_1) + \lambda_4 W(s_1, t) > y - \lambda_1 r_1 - \lambda_2 r_2 | R_1 = r_1, R_2 = r_2) \\
&\quad \cdot P(\lambda_3 R_3(s_2) + \lambda_4 W(s_2, t) > y - \lambda_1 r_1 - \lambda_2 r_2 | R_1 = r_1, R_2 = r_2) I(\lambda_1 r_1 + \lambda_2 r_2 < y)\}]
\end{aligned} \tag{8}$$

Since $\lambda_1 R_1 + \lambda_2 R_2$ follows a hypoexponential distribution with parameters λ_1, λ_2 , we know

$$P(\lambda_1 R_1 + \lambda_2 R_2 > y) = \frac{\lambda_1}{\lambda_1 - \lambda_2} \exp(-x/\lambda_1) - \frac{\lambda_2}{\lambda_1 - \lambda_2} \exp(-x/\lambda_2).$$

Next, consider the the second term in equation (2).

$$\begin{aligned} & E_{R_1} [E_{R_2} \{P(\lambda_3 R_3(s_1) + \lambda_4 W(s_1, t) > y - \lambda_1 r_1 - \lambda_2 r_2 | R_1 = r_1, R_2 = r_2)^2 I(\lambda_1 r_1 + \lambda_2 r_2 < y)\}] \\ &= E_{R_1} \left\{ E_{R_2} \left(\left[\frac{\lambda_3}{\lambda_3 - \lambda_4} \exp \left\{ \frac{-(y - \lambda_1 r_1 - \lambda_2 r_2)}{\lambda_3} \right\} - \frac{\lambda_4}{\lambda_3 - \lambda_4} \exp \left\{ \frac{-(y - \lambda_1 r_1 - \lambda_2 r_2)}{\lambda_4} \right\} \right]^2 I[\lambda_1 r_1 + \lambda_2 r_2 < y] \right) \right\} \\ &= \int_0^{y/\lambda_1} \int_0^{(y-\lambda_1 r_1)/\lambda_2} \left[\left\{ \frac{\lambda_3}{\lambda_3 - \lambda_4} \right\}^2 \exp \left\{ \frac{-2(y - \lambda_1 r_1 - \lambda_2 r_2)}{\lambda_3} \right\} + \left\{ \frac{\lambda_4}{\lambda_3 - \lambda_4} \right\}^2 \exp \left\{ \frac{-2(y - \lambda_1 r_1 - \lambda_2 r_2)}{\lambda_4} \right\} \right. \\ &\quad \left. - 2 \left\{ \frac{\lambda_3 \lambda_4}{(\lambda_3 - \lambda_4)^2} \right\} \exp \left\{ - \left(\frac{1}{\lambda_3} + \frac{1}{\lambda_4} \right) (y - \lambda_1 r_1 - \lambda_2 r_2) \right\} \right] e^{-r_2} dr_2 e^{-r_1} dr_1 \\ &= I_1 + I_2 + I_3 \end{aligned}$$

The first line is obtained by noting that $\lambda_3 R_3(s_1) + \lambda_4 W(s_1, t)$ and $\lambda_3 R_3(s_2) + \lambda_4 W(s_2, t)$ are identically distributed. The second line is obtained by substituting the hypoexponential survival function.

We can separate this integral into three additive pieces, I_1, I_2, I_3 , and handle them individually.

$$\begin{aligned} I_1 &= \left\{ \frac{\lambda_3}{\lambda_3 - \lambda_4} \right\}^2 \int_0^{y/\lambda_1} \exp \left\{ \frac{-2(y - \lambda_1 r_1)}{\lambda_3} \right\} \left\{ \int_0^{(y-\lambda_1 r_1)/\lambda_2} \left[\exp \left\{ \left(\frac{2\lambda_2}{\lambda_3} - 1 \right) r_2 \right\} \right] dr_2 \right\} e^{-r_1} dr_1 \\ &= \left\{ \frac{\lambda_3}{\lambda_3 - \lambda_4} \right\}^2 \frac{\lambda_3}{2\lambda_2 - \lambda_3} \int_0^{y/\lambda_1} \left[\exp \left\{ \frac{-2(y - \lambda_1 r_1)}{\lambda_3} \right\} \exp \left\{ \left(\frac{2}{\lambda_3} - \frac{1}{\lambda_2} \right) (y - \lambda_1 r_1) \right\} - 1 \right] e^{-r_1} dr_1 \\ &= \left\{ \frac{\lambda_3}{\lambda_3 - \lambda_4} \right\}^2 \frac{\lambda_3}{2\lambda_2 - \lambda_3} \left[\frac{\lambda_2}{\lambda_1 - \lambda_2} \left\{ \exp \left(- \frac{y}{\lambda_1} \right) - \exp \left(- \frac{y}{\lambda_2} \right) \right\} - \frac{\lambda_3}{2\lambda_1 - \lambda_3} \left\{ \exp \left(- \frac{y}{\lambda_1} \right) - \exp \left(- \frac{2y}{\lambda_3} \right) \right\} \right] \end{aligned}$$

For brevity I skip the steps for integration for the second and third integrands in equation (3). The results are below:

$$\begin{aligned}
I_1 &= \int_0^{y/\lambda_1} \int_0^{(y-\lambda_1 r_1)/\lambda_2} \left[\left\{ \frac{\lambda_3}{\lambda_3 - \lambda_4} \right\}^2 \exp\{-2\lambda_3^{-1}(y - \lambda_1 r_1 - \lambda_2 r_2)\} \right] e^{-r_2} dr_2 e^{-r_1} dr_1 \\
&= \left(\frac{\lambda_3}{\lambda_3 - \lambda_4} \right)^2 \frac{\lambda_3}{2\lambda_2 - \lambda_3} \left[\frac{\lambda_2}{\lambda_1 - \lambda_2} \{ \exp(-\lambda_1^{-1}y) - \exp(-\lambda_2^{-1}y) \} - \frac{\lambda_3}{2\lambda_1 - \lambda_3} \{ \exp(-\lambda_1^{-1}y) - \exp(-2\lambda_3^{-1}y) \} \right] \\
I_2 &= \int_0^{y/\lambda_1} \int_0^{(y-\lambda_1 r_1)/\lambda_2} \left\{ \frac{\lambda_4}{\lambda_3 - \lambda_4} \right\}^2 \exp\{-2\lambda_4^{-1}(y - \lambda_1 r_1 - \lambda_2 r_2)\} e^{-r_2} dr_2 e^{-r_1} dr_1 \\
&= \left(\frac{\lambda_4}{\lambda_3 - \lambda_4} \right)^2 \frac{\lambda_4}{2\lambda_2 - \lambda_4} \left[\frac{\lambda_2}{\lambda_1 - \lambda_2} \{ \exp(-\lambda_1^{-1}y) - \exp(-\lambda_2^{-1}y) \} - \frac{\lambda_4}{2\lambda_1 - \lambda_4} \{ \exp(-\lambda_1^{-1}y) - \exp(-2\lambda_4^{-1}y) \} \right] \\
I_3 &= \int_0^{y/\lambda_1} \int_0^{(y-\lambda_1 r_1)/\lambda_2} -2 \frac{\lambda_3 \lambda_4}{(\lambda_3 - \lambda_4)^2} \exp\{-(\lambda_3^{-1} + \lambda_4^{-1})(y - \lambda_1 r_1 - \lambda_2 r_2)\} e^{-r_2} dr_2 e^{-r_1} dr_1 \\
&= -2 \frac{\lambda_3 \lambda_4}{(\lambda_3 - \lambda_4)^2} \frac{\lambda_3 \lambda_4}{\lambda_2(\lambda_3 + \lambda_4) - \lambda_3 \lambda_4} \left[\frac{\lambda_2}{\lambda_1 - \lambda_2} \{ \exp(-\lambda_1^{-1}y) - \exp(-\lambda_2^{-1}y) \} \right. \\
&\quad \left. - \frac{\lambda_3 \lambda_4}{\lambda_1(\lambda_3 + \lambda_4) - \lambda_3 \lambda_4} \{ \exp(-\lambda_1^{-1}y) - \exp(-(\lambda_3^{-1} + \lambda_4^{-1})y) \} \right]
\end{aligned}$$

Gathering terms and simplifying gives $P(X_1 > y, X_2 > y) = c_1 e^{-y/\lambda_1} + c_2 e^{-y/\lambda_2} + c_3 e^{-2y/\lambda_3} + c_4 e^{-2y/\lambda_4} + c_5 e^{-(y/\lambda_3 + y/\lambda_4)}$ where

$$\begin{aligned}
c_1 &= \frac{\lambda_1}{(\lambda_1 - \lambda_2)} + \frac{\lambda_1 \lambda_3^3}{(\lambda_1 - \lambda_2)(\lambda_3 - \lambda_4)^2(2\lambda_1 - \lambda_3)} + \frac{\lambda_1 \lambda_4^3}{(\lambda_1 - \lambda_2)(\lambda_3 - \lambda_4)^2(2\lambda_1 - \lambda_4)} \\
&\quad - \frac{2\lambda_1 \lambda_3^2 \lambda_4^2}{(\lambda_1 - \lambda_2)(\lambda_3 - \lambda_4)^2(\lambda_1 \lambda_3 + \lambda_1 \lambda_4 - \lambda_3 \lambda_4)} \\
c_2 &= -\frac{\lambda_2}{(\lambda_1 - \lambda_2)} - \frac{\lambda_2 \lambda_3^3}{(\lambda_1 - \lambda_2)(\lambda_3 - \lambda_4)^2(2\lambda_2 - \lambda_3)} - \frac{\lambda_2 \lambda_4^3}{(\lambda_1 - \lambda_2)(\lambda_3 - \lambda_4)^2(2\lambda_2 - \lambda_4)} \\
&\quad + \frac{2\lambda_2 \lambda_3^2 \lambda_4^2}{(\lambda_1 - \lambda_2)(\lambda_3 - \lambda_4)^2(\lambda_2 \lambda_3 + \lambda_2 \lambda_4 - \lambda_3 \lambda_4)} \\
c_3 &= \frac{\lambda_3^4}{(\lambda_3 - \lambda_4)^2(2\lambda_1 - \lambda_3)(2\lambda_2 - \lambda_3)} \\
c_4 &= \frac{\lambda_4^4}{(\lambda_3 - \lambda_4)^2(2\lambda_1 - \lambda_4)(2\lambda_2 - \lambda_4)} \\
c_5 &= \frac{-2\lambda_3^3 \lambda_4^3}{(\lambda_3 - \lambda_4)^2(\lambda_2 \lambda_3 + \lambda_2 \lambda_4 - \lambda_3 \lambda_4)(\lambda_1 \lambda_3 + \lambda_1 \lambda_4 - \lambda_3 \lambda_4)}
\end{aligned}$$

Now, we have an expression for $P(X_1 > y, X_2 > y)$. Additionally, since X_1 follows a 4-parameter hypoexponential distribution, we have:

$$P(X_1 > y) = \sum_{i=1}^4 \exp(-\lambda_i^{-1}y) \prod_{1 \leq j \leq 4, j \neq i} \left(\frac{\lambda_i}{\lambda_i - \lambda_j} \right)$$

Then, if the index of the largest λ_i , $\text{argmax}_i \lambda_i = 3$ or 4 , $\lim_{y \rightarrow \infty} P(X_1 > y, X_2 > y) / P(X_1 >$

$y) = 0$ so X_1 and X_2 will be asymptotically independent. Otherwise, if $\operatorname{argmax}_i \lambda_i = 1$ or 2, then X_1 and X_2 will be asymptotically dependent and the limit $\chi(X_1, X_2)$ will be $c_j \prod_{1 \leq l \leq 4, l \neq j} \left(\frac{\lambda_j}{\lambda_j - \lambda_l}\right)^{-1}$ where $j = \operatorname{argmax}_i \lambda_i$ and c_i is as defined above.

This result holds if c_1, c_2 are non-zero. To verify this, I expand the numerator terms of c_1, c_2 and find the roots of the resulting polynomial in Wolfram Alpha. None of the roots occurred in the restricted domain we proposed for λ_i , so we conclude this is not a concern.

Case 2: $s_1 = s_2, t_1 \neq t_2$

This case mirrors the proof above, so I will not include it for brevity.

We find that if the index of the largest λ_i , $\operatorname{argmax}_i \lambda_i = 2$ or 4, $\lim_{y \rightarrow \infty} P(X_1 > y, X_2 > y) / P(X_1 > y) = 0$ so X_1 and X_2 will be asymptotically independent. Otherwise, if $\operatorname{argmax}_i \lambda_i = 1$ or 3, then X_1 and X_2 will be asymptotically dependent and the limit $\chi(X_1, X_2)$ will be $c_j \prod_{1 \leq l \leq 4, l \neq j} \left(\frac{\lambda_j}{\lambda_j - \lambda_l}\right)^{-1}$ where $j = \operatorname{argmax}_i \lambda_i$ and c_i is as defined above.

Case 3: $s_1 \neq s_2, t_1 \neq t_2$

We have $X_1 = \lambda_1 R_1 + \lambda_2 R_2(t_1) + \lambda_3 R_3(s_1) + \lambda_4 W(s_1, t_1)$, $X_2 = \lambda_1 R_1 + \lambda_2 R_2(t_2) + \lambda_3 R_3(s_2) + \lambda_4 W(s_2, t_2)$.

Then, we have the following:

$$\begin{aligned} P(X_1 > y, X_2 > y) &= P(\lambda_1 R_1 + \lambda_2 R_2 + \lambda_3 R_3(s_1) + \lambda_4 W(s_1, t) > y, \lambda_1 R_1 + \lambda_2 R_2 + \lambda_3 R_3(s_2) \\ &\quad + \lambda_4 W(s_2, t) > y) \\ &= E_{R_1} \{ P(\lambda_2 R_2(t_1) + \lambda_3 R_3(s_1) + \lambda_4 W(s_1, t_1) > y - \lambda_1 r_1, \lambda_2 R_2(t_2) + \lambda_3 R_3(s_2) \\ &\quad + \lambda_4 W(s_2, t_2) > y - \lambda_1 r_1 | R_1 = r_1) \} \\ &= P(R_1 > y/\lambda_1) + \int_0^{y/\lambda_1} P(\lambda_2 R_2 + \lambda_3 R_3 + \lambda_4 W > y - \lambda_1 r)^2 e^{-r} dr \end{aligned}$$

Since R_1 follows a standard exponential distribution, $P(R_1 > y/\lambda_1) = \exp(-y/\lambda_1)$. Since $\lambda_2 R_2 + \lambda_3 R_3 + \lambda_4 W$ follows a hypoexponential distribution with parameters $\lambda_2, \lambda_3, \lambda_4$, we know:

$$P(\lambda_2 R_2 + \lambda_3 R_3 + \lambda_4 W > x) = \left\{ \frac{\lambda_2^2 \exp(-y/\lambda_2)}{(\lambda_2 - \lambda_3)(\lambda_2 - \lambda_4)} - \frac{\lambda_3^2 \exp(-y/\lambda_3)}{(\lambda_2 - \lambda_3)(\lambda_3 - \lambda_4)} + \frac{\lambda_4^2 \exp(-y/\lambda_4)}{(\lambda_2 - \lambda_4)(\lambda_3 - \lambda_4)} \right\}$$

if $x > 0$, and 1 otherwise.

The expression in the integral can be expanded as follows:

$$\begin{aligned}
& \int_0^{y/\lambda_1} P(\lambda_2 R_2 + \lambda_3 R_3 + \lambda_4 W > y - \lambda_1 r)^2 e^{-r} dr \\
&= \int_0^{y/\lambda_1} \left[\frac{\lambda_2^2 \exp\{-\lambda_2^{-1}(y - \lambda_1 r)\}}{(\lambda_2 - \lambda_3)(\lambda_2 - \lambda_4)} - \frac{\lambda_3^2 \exp\{-\lambda_3^{-1}(y - \lambda_1 r)\}}{(\lambda_2 - \lambda_3)(\lambda_3 - \lambda_4)} + \frac{\lambda_4^2 \exp\{-\lambda_4^{-1}(y - \lambda_1 r)\}}{(\lambda_2 - \lambda_4)(\lambda_3 - \lambda_4)} \right]^2 e^{-r} dr \\
&= \int_0^{y/\lambda_1} \left[\frac{\lambda_2^4 \exp\{-2\lambda_2^{-1}(y - \lambda_1 r)\}}{(\lambda_2 - \lambda_3)^2(\lambda_2 - \lambda_4)^2} + \frac{-\lambda_3^4 \exp\{-2\lambda_3^{-1}(y - \lambda_1 r)\}}{(\lambda_2 - \lambda_3)^2(\lambda_3 - \lambda_4)^2} + \frac{-\lambda_4^4 \exp\{-2\lambda_4^{-1}(y - \lambda_1 r)\}}{(\lambda_2 - \lambda_4)^2(\lambda_3 - \lambda_4)^2} \right. \\
&\quad - \frac{2\lambda_2^2 \lambda_3^2 \exp\{-(y - \lambda_1 r)(\lambda_2^{-1} + \lambda_3^{-1})\}}{(\lambda_2 - \lambda_3)^2(\lambda_2 - \lambda_4)(\lambda_3 - \lambda_4)} - \frac{2\lambda_3^2 \lambda_4^2 \exp\{-(y - \lambda_1 r)(\lambda_3^{-1} + \lambda_4^{-1})\}}{(\lambda_3 - \lambda_4)^2(\lambda_2 - \lambda_3)(\lambda_2 - \lambda_4)} \\
&\quad \left. + \frac{2\lambda_2^2 \lambda_4^2 \exp\{-(y - \lambda_1 r)(\lambda_2^{-1} + \lambda_4^{-1})\}}{(\lambda_2 - \lambda_4)^2(\lambda_2 - \lambda_3)(\lambda_3 - \lambda_4)} \right] e^{-r} dr \\
&= J_1 + J_2 + J_3 + J_4 + J_5 + J_6
\end{aligned}$$

We can split this integral additively and evaluate each piece separately.

$$\begin{aligned}
J_1 &= \int_0^{y/\lambda_1} \frac{\lambda_2^4 \exp\{-2\lambda_2^{-1}(y - \lambda_1 r)\}}{(\lambda_2 - \lambda_3)^2(\lambda_2 - \lambda_4)^2} e^{-r} dr \\
&= \frac{\lambda_2^4 \exp(-2\lambda_2^{-1}y)}{(\lambda_2 - \lambda_3)^2(\lambda_2 - \lambda_4)^2} \int_0^{y/\lambda_1} \exp\left\{\left(\frac{2\lambda_1}{\lambda_2} - 1\right)r\right\} dr \\
&= \frac{\lambda_2^4 \exp(-2\lambda_2^{-1}y)}{(\lambda_2 - \lambda_3)^2(\lambda_2 - \lambda_4)^2} \left[\frac{\exp\{(2\lambda_2^{-1} - \lambda_1^{-1})y\} - 1}{\frac{2\lambda_1}{\lambda_2} - 1} \right] \\
&= \frac{\lambda_2^5 \{\exp(-\lambda_1^{-1}y) - \exp(-2\lambda_2^{-1}y)\}}{(\lambda_2 - \lambda_3)^2(\lambda_2 - \lambda_4)^2(2\lambda_1 - \lambda_2)}
\end{aligned}$$

For brevity I skip the steps for integration for the other five terms.

$$\begin{aligned}
J_2 &= \int_0^{y/\lambda_1} \frac{\lambda_3^4 \exp\{-2(y - \lambda_1 r)/\lambda_3\}}{(\lambda_2 - \lambda_3)^2(\lambda_3 - \lambda_4)^2} e^{-r} dr = \frac{\lambda_3^5 \{\exp(-y/\lambda_1) - \exp(-2y/\lambda_3)\}}{(\lambda_2 - \lambda_3)^2(\lambda_3 - \lambda_4)^2(2\lambda_1 - \lambda_2)} \\
J_3 &= \int_0^{y/\lambda_1} \frac{\lambda_4^4 \exp\{-2(y - \lambda_1 r)/\lambda_4\}}{(\lambda_2 - \lambda_4)^2(\lambda_3 - \lambda_4)^2} e^{-r} dr = \frac{\lambda_4^5 \{\exp(-y/\lambda_1) - \exp(-2y/\lambda_4)\}}{(\lambda_2 - \lambda_4)^2(\lambda_3 - \lambda_4)^2(2\lambda_1 - \lambda_4)} \\
J_4 &= \int_0^{y/\lambda_1} \frac{2\lambda_2^2 \lambda_3^2 \exp\{-(y - \lambda_1 r)(\lambda_2^{-1} + \lambda_3^{-1})\}}{(\lambda_2 - \lambda_3)^2(\lambda_2 - \lambda_4)(\lambda_3 - \lambda_4)} e^{-r} dr \\
&= \frac{2\lambda_2^3 \lambda_3^3 [\exp\{-y/\lambda_1\} - \exp\{-y(\lambda_2^{-1} + \lambda_3^{-1})\}]}{(\lambda_2 - \lambda_3)^2(\lambda_2 - \lambda_4)(\lambda_3 - \lambda_4)(\lambda_1 \lambda_2 + \lambda_1 \lambda_3 - \lambda_2 \lambda_3)} \\
J_5 &= \int_0^{y/\lambda_1} \frac{2\lambda_2^2 \lambda_4^2 \exp\{-(y - \lambda_1 r)(\lambda_2^{-1} + \lambda_4^{-1})\}}{(\lambda_2 - \lambda_4)^2(\lambda_2 - \lambda_3)(\lambda_3 - \lambda_4)} e^{-r} dr \\
&= \frac{2\lambda_2^3 \lambda_4^3 [\exp\{-y/\lambda_1\} - \exp\{-y(\lambda_2^{-1} + \lambda_4^{-1})\}]}{(\lambda_2 - \lambda_4)^2(\lambda_2 - \lambda_3)(\lambda_3 - \lambda_4)(\lambda_1 \lambda_2 + \lambda_1 \lambda_4 - \lambda_2 \lambda_4)} \\
J_6 &= \int_0^{y/\lambda_1} \frac{2\lambda_3^2 \lambda_4^2 \exp\{-(y - \lambda_1 r)(\lambda_3^{-1} + \lambda_4^{-1})\}}{(\lambda_3 - \lambda_4)^2(\lambda_2 - \lambda_3)(\lambda_2 - \lambda_4)} e^{-r} dr \\
&= \frac{2\lambda_3^3 \lambda_4^3 [\exp\{-y/\lambda_1\} - \exp\{-y(\lambda_3^{-1} + \lambda_4^{-1})\}]}{(\lambda_3 - \lambda_4)^2(\lambda_2 - \lambda_3)(\lambda_2 - \lambda_4)(\lambda_1 \lambda_3 + \lambda_1 \lambda_4 - \lambda_3 \lambda_4)}
\end{aligned}$$

We can see the joint survival probability is $c_1 \exp(-y/\lambda_1) + c_2 \exp(-2y/\lambda_2) + c_3 \exp(-2y/\lambda_3) + c_4 \exp(-2y/\lambda_4) + c_5 \exp\{-y(\lambda_2^{-1} + \lambda_3^{-1})\} + c_6 \exp\{-y(\lambda_2^{-1} + \lambda_4^{-1})\} + c_7 \exp\{-y(\lambda_3^{-1} + \lambda_4^{-1})\}$ where

$$\begin{aligned}
c_1 &= - \sum_{i=2}^7 c_i \\
c_2 &= \frac{-\lambda_2^5}{(\lambda_2 - \lambda_3)^2(\lambda_2 - \lambda_4)^2(2\lambda_1 - \lambda_2)} \\
c_3 &= \frac{-\lambda_3^5}{(\lambda_2 - \lambda_3)^2(\lambda_3 - \lambda_4)^2(2\lambda_1 - \lambda_3)} \\
c_4 &= \frac{-\lambda_4^5}{(\lambda_2 - \lambda_4)^2(\lambda_3 - \lambda_4)^2(2\lambda_1 - \lambda_4)} \\
c_5 &= \frac{2\lambda_2^3 \lambda_3^3}{(\lambda_2 - \lambda_3)^2(\lambda_2 - \lambda_4)(\lambda_3 - \lambda_4)(\lambda_1 \lambda_2 + \lambda_1 \lambda_3 - \lambda_2 \lambda_3)} \\
c_6 &= \frac{-2\lambda_2^3 \lambda_4^3}{(\lambda_2 - \lambda_4)^2(\lambda_2 - \lambda_3)(\lambda_3 - \lambda_4)(\lambda_1 \lambda_2 + \lambda_1 \lambda_4 - \lambda_2 \lambda_4)} \\
c_7 &= \frac{2\lambda_3^3 \lambda_4^3}{(\lambda_3 - \lambda_4)^2(\lambda_2 - \lambda_3)(\lambda_2 - \lambda_4)(\lambda_1 \lambda_3 + \lambda_1 \lambda_4 - \lambda_3 \lambda_4)}
\end{aligned}$$

Additionally, since X_1 follows a four-parameter hypoexponential distribution, we have:

$$P(X_1 > y) = \sum_{i=1}^4 \exp(-\lambda_i^{-1} y) \prod_{1 \leq j \leq 4, j \neq i} \left(\frac{\lambda_i}{\lambda_i - \lambda_j} \right)$$

Then, it is clear that $\lim_{y \rightarrow \infty} P(X_1 > y, X_2 > y)/P(X_1 > y) = 0$ only when $\text{argmax}_i \lambda_i \neq$

1, so it will be asymptotically independent. Otherwise, X_1 and X_2 will be asymptotically dependent, and the limit χ will be:

$$\frac{c_1}{\prod_{2 \leq j \leq 4} \left(\frac{\lambda_i}{\lambda_1 - \lambda_j} \right)}$$

the ratio of coefficients of the $\exp(-y/\lambda_1)$ terms derived in the previous steps.